Risk Group Turnover in Epidemic Models

Jesse Knight[a], Stefan Baral[b], Sheree Schwartz[b], Linwei Wang[a], Huiting Ma[a], Katherine Young[c], Harry Hausler[c], Sharmistha Mishra[a,d,e,f,*]

[a] *MAP Centre for Urban Health Solutions, Unity Health Toronto*
[b] *Deptartment of Epidemiology, Johns Hopkins Bloomberg School of Public Health*
[c] *TB HIV Care, South Africa*
[d] *Department of Medicine, Division of Infectious Disease, University of Toronto*
[e] *Institute of Health Policy, Management and Evaluation, Dalla Lana School of Public Health, University of Toronto*
[f] *Instituof Medical Sciences, University of Toronto*

Abstract

Background. Epidemic models are often used to estimate the contribution of high risk groups to the overall epidemic, helping to inform intervention priorities. While many epidemic models stratify populations by heterogeneity in risk, few consider movement of individuals between risk groups, which we call turnover. Its not clear how turnover can be modelled based on epidemiologic data, or how inclusion of turnover in epidemic models will influence the projected importance of interventions reaching high risk groups. Methods. We developed a framework for modelling risk group turnover in deterministic compartmental transmission models which incorporates available data and assumptions as constraints. We applied this framework to an illustrative STI/HIV model to examine the influence of turnover on: the equilibrium infection prevalence and incidence across risk groups; the inferred level of risk heterogeneity; and the importance of interventions reaching the highest risk group. Results. The equilibrium prevalence ratio between the highest and lowest risk groups decreased with increasing rates of turnover. The level of risk heterogeneity inferred via model fitting to the same prevalence targets was then higher with turnover than without. After model fitting, the estimated importance of interventions reaching the highest risk group was also higher with turnover than without. Implications. Equilibrium prevalence predicted by epidemic models can be strongly influenced by turnover. The projected importance of interventions prioritizing on high risk groups could be underestimated if fitted models do not simulate turnover which is present in reality. Collection of data which can be used to parameterize risk group turnover in epidemic models should be prioritized.

Keywords: mathematical modelling, risk heterogeneity, STI, HIV

* Corresponding author (sharmistha.mishra@unityhealth.to.ca)

Abbreviations: HIV: human immunodeficiency virus, TPAF: transmission population attributable fraction

Contents

1 Introduction **1**

2 Methods **2**

2.1 Turnover System 2

2.2 Model & Simulations 3

2.3 Experiments 6

3 Results **8**

3.1 Experiment 1: How turnover influences equilibrium incidence and prevalence 8

3.2 Experiment 2: Inferred risk heterogeneity with vs without turnover 11

3.3 Experiment 3: Influence of turnover on the TPAF of the highest risk group 11

4 Discussion **12**

A Turnover System **19**

A.1 Notation 19

A.2 Parameterization 19

A.3 Previous Approaches 24

B Supplemental Equations **27**

B.1 Model Equations 27

B.2 Complete Example Turnover System 28

B.3 Redundancy in specifying all elements of $\hat{e}$ 28

B.4 Factors of Incidence 28

C Supplemental Results **30**

C.1 Equilibrium Incidence 30

C.2 Equilibrium Incidence Ratios 30

C.3 Equilibrium prevalence before and after model fitting 31

C.4 Contact rate before and after model fitting 32

C.5 Influence of turnover on the TPAF of the highest risk group before model fitting 33

C.6 Distribution of health states at equilibrium 34

C.7 Rates of transition at equilibrium 35

C.8 New infections from turnover vs incidence 36

1. Introduction

Heterogeneity in transmission risk is a consistent characteristic of epidemics of sexually transmitted infections (STI) (Anderson and May, 1991). This heterogeneity is often demarcated by identifying specific populations whose risks of acquisition and onward transmission of STI are the highest, such that their specific unmet prevention and treatment needs can sustain local epidemics of STI (Yorke et al., 1978). Increased risk can be conferred in many ways, including a higher number of sexual partners, reduced condom use, stigma during access to care. The contribution of high risk groups to the overall epidemic can then be used as an indicator in the appraisal of STI epidemics, helping to guide intervention priorities (Shubber et al., 2014; Mishra et al., 2016).

Traditionally, contribution has been quantified using the *population attributable fraction* (PAF): the proportion of new infections which are attributable to disproportionate risk of transmission in a given population, such as in the modes of transmission model (Case et al., 2012; Mishra et al., 2014). However, transmission models are increasingly being used to quantify contribution over longer time horizons using the *transmission population attributable fraction* (TPAF). The TPAF is estimated by simulating counterfactual scenarios where transmission between specific subgroups is stopped, and the relative difference in cumulative infections in the total population over various time-periods is measured (Mishra et al., 2016; Mukandavire et al., 2018). Transmission can be stopped by setting susceptibility and/or infectiousness to zero in the model (Mishra et al., 2012). The TPAF is then interpreted as the fraction of all new infections that stem, directly and indirectly, from a failure to prevent acquisition and/or to provide effective treatment in a particular risk group (Mishra et al., 2016).

An epidemiologic phenomenon that is sometimes missing from transmission models, but is well-described in the context of sexual behaviour, is the movement of individuals between risk groups. Such movement is often referred to in the STI epidemiology literature as *turnover* (Watts et al., 2010). For example, turnover may reflect entry into or retirement from formal sex work, or other periods associated with higher STI susceptibility and onward transmission due to more partners and/or vulnerabilities (Marston and King, 2006; Watts et al., 2010). Risk group turnover has been shown to influence the predicted equilibrium prevalence of an STI (Stigum et al., 1994; Zhang et al., 2012); the fraction of transmissions occurring during acute HIV infection (Zhang et al., 2012); the basic reproductive number R_0 (Henry and Koopman, 2015); and the coverage of antiretroviral therapy required to achieve HIV epidemic control (Henry and Koopman, 2015). Yet how, and the extent to which, turnover influences TPAF remains unknown. Implementations of risk group turnover in compartmental transmission models also vary widely. In some simple models, the rates of movement between two risk groups is balanced analytically based on the sizes of the groups (Koopman et al., 1997; Stigum et al., 1994). In more complex models, a stabilization period is used to equilibrate turnover dynamics, during which time the sizes of risk groups may deviate from their initial

values (Boily et al., 2015). Other models only consider unidirectional turnover – e.g. from high to low risk (Eaton and Hallett, 2014).

Challenges in implementing turnover include incorporation of data-driven epidemiologic constraints. For example, data may suggest that the relative sizes of specific populations in the model, such as the population of sex workers, have remained constant over time. Data may also suggest that heterogeneity in risk behaviour of individuals entering into the model (reflecting coital debut) may be different from the risk behaviour of individuals already in the model (reflecting sexually active adults). Data may indicate the average duration of a high risk period of one's sexual life-course (Watts et al., 2010), or how their behaviour changes following that period. Such data should be reflected in implementations of turnover, but it is not always clear how to do so. Moreover, without an exact analysis of the turnover implementation, a burn-in period may be required to equilibrate the system, resulting in potentially unwanted changes to the initial group sizes.

In this paper, we aim to examine the influence of risk group turnover on the TPAF of a high risk group in an illustrative STI without STI-attributable mortality. First, we propose a solution to the challenges outlined above of parameterizing turnover based on epidemiologic data while avoiding the need for an equilibration period. We then examine the mechanisms by which turnover influences group-specific STI prevalence (Experiment 1). Next, we examine how inclusion/exclusion of turnover influences the values of heterogeneity-related parameters inferred during model fitting (Experiment 2). Finally, we compare the TPAF of the highest risk group estimated by two models after fitting to same setting: one model with and one model without turnover (Experiment 3).

2. Methods

We aimed to determine and understand the influence of risk group turnover on the contribution of the highest risk group to the overall epidemic, as measured by the transmission population attributable fraction (TPAF). This section introduces a new framework for parameterizing turnover, describes the STI model used in the experiments, and outlines the experiments.

2.1. Turnover System

We developed a framework for modelling turnover, based on the system shown in Figure 1. A more detailed description of this framework is given in Appendix A. The simulated population is divided into G risk groups. The number of individuals in group $i \in [1, \ldots, G]$ is denoted x_i, and the relative size of each group is denoted $\hat{x}_i = x_i/N$, where N is the total population size. Individuals enter the population at a rate ν and exit at a rate μ per year. The distribution of risk groups among individuals entering into the model is denoted $\hat{e}_i$, which may be different from $\hat{x}_i$. The total number of individuals entering into group i per year is therefore given by $\nu \hat{e}_i N$. Turnover rates are collected in a $G \times G$ matrix ϕ, where ϕ_{ij} is the proportion

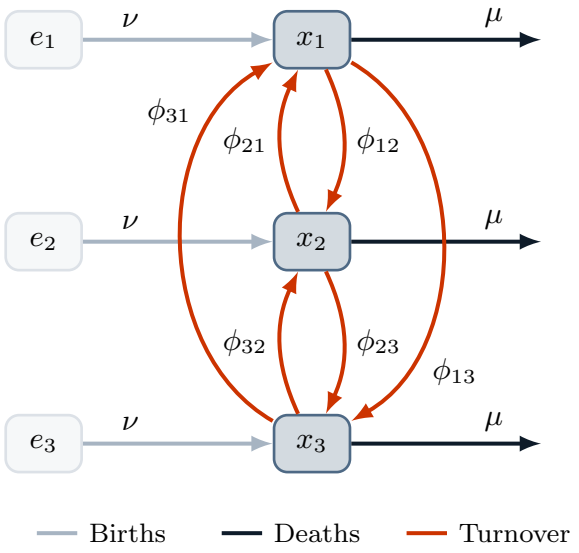

Figure 1: System of risk groups and flows between them for $G = 3$

of individuals in group i who move from group i into group j each year. We assume that rates of turnover ϕ are not affected by the health state of individuals.

We assume that the relative sizes of risk groups in the model $\hat{\boldsymbol{x}} = [\hat{x}_1, \ldots, \hat{x}_G]$ are known and should remain constant over time. We also assume that the rates of population entry ν and exit μ are known, but that they may vary over time. Methods to estimate ν and μ are given in Appendix A.2.1. What remains is to estimate $\hat{\boldsymbol{e}}$ and ϕ, representing $G + G(G-1) = G^2$ unknown values. In the proposed framework, these variables are collected in the vector $\boldsymbol{\theta} = [\hat{\boldsymbol{e}}, \boldsymbol{y}]$, where $\boldsymbol{y} = \text{vec}_{i \neq j}(\phi)$. We then construct a set of linear constraints based on data to uniquely determine the elements of $\boldsymbol{\theta}$. Using this approach, each constraint k takes the form $b_k = A_k \boldsymbol{\theta}$, where b_k is a constant and A_k is a vector with the same length as $\boldsymbol{\theta}$. The values of $\boldsymbol{\theta}$ can then be obtained by solving $\boldsymbol{\theta} = A^{-1}\boldsymbol{b}$, for which many algorithms exist (LAPACK, 1992).

We define four types of constraints which can used to solve for the values of $\hat{\boldsymbol{e}}$ and ϕ via $\boldsymbol{\theta}$. These constraints can be selected and combined together in a flexible way, depending on the availability of data and plausibility of assumptions. However, a minimum of G^2 non-redundant constraints must be specified to ensure a "unique solution" – exactly one value of $\boldsymbol{\theta}$ which satisfies all constraints. The four types of constraints, and the data to required to define them, are summarized in Table 1. Additional details, including constraint equations, examples, and considerations for combining constraints, are given in Appendix A.2.2.

2.2. Model & Simulations

To run our experiments, we developed a deterministic single-sex susceptible-infectious-treated (SIT) model which simulates transmission in a population with heterogeneity in risk. The model is not representative of a specific infection but includes transmission via partnerships as per sexually transmitted infections

Table 1: Summary of constraint types for defining risk group turnover

Name	Description	Variables	Data sources & Examples
1. Constant group size	the relative sizes of groups are known or assumed, and assumed to not change over time	$\hat{x}_i$	demographic health surveys (USAID, 2019), key population mapping and enumeration (Abdul-Quader et al., 2014)
2. Specified elements	group sizes in the population following sexual debut and/or individual rates of turnover are known or assumed	$\hat{e}_i$, ϕ_{ij}	demographic health surveys (USAID, 2019), key population surveys (Baral et al., 2014)
3. Group duration	the average durations of individuals in each group are known or assumed	δ_i	cohort studies of sexual behaviour over time (Fergus et al., 2007), key population surveys (Baral et al., 2014)
4. Turnover rate ratios	ratios between different rates of turnover are known or assumed	ϕ_{ij}	demographic health surveys (USAID, 2019), key population surveys (Baral et al., 2014)

ν: rate of population entry; ϕ_{ij}: rate of turnover from group i to group j; $\hat{x}_i$: proportion of individuals in risk group i; $\hat{e}_i$: proportion of individuals entering into risk group i; δ_i: average duration spent in risk group i.

Figure 2: Modelled health states. $\mathcal{S}$: susceptible; $\mathcal{I}$: infected; $\mathcal{T}$: treated; λ: force of infection; τ: treatment.

(Garnett and Anderson, 1994). The model includes three health states: susceptible $\mathcal{S}$, infectious $\mathcal{I}$, and treated $\mathcal{T}$ (Figure 2), and $G = 3$ levels of risk: high H, medium M, and low L. Risk strata are defined by different number of contacts per year so that individuals in risk group i are assumed to form contacts at a rate C_i per year. The probability of contact formation ρ_{ik} between individuals in group i and individuals in risk group k is assumed to be proportionate to the total number of available contacts within each group:

$$\rho_{ik} = \frac{C_k x_k}{\sum_{\mathrm{k}} C_{\mathrm{k}} x_{\mathrm{k}}} \tag{1}$$

The biological probability of transmission is defined as β per contact. Individuals transition from the susceptible $\mathcal{S}$ to infectious $\mathcal{I}$ health-state via a force of infection λ per year, per susceptible in risk group i:

$$\lambda_i = C_i \sum_k \rho_{ik}\, \beta\, \frac{\mathcal{I}_k}{x_k} \tag{2}$$

Individuals are assumed to transition from the infectious $\mathcal{I}$ to treated $\mathcal{T}$ health-state at a rate τ per year, reflecting diagnosis and treatment. The treatment rate is not stratified by risk group. Individuals in the treated $\mathcal{T}$ health-state are not infectious nor susceptible, and individuals cannot become re-infected.

2.2.1. Turnover implementation

As described in Section 2.1, individuals enter the model at a rate ν, exit the model at a rate μ, and transition from risk group i to group j at a rate ϕ_{ij}. The turnover rates ϕ and distribution of individuals

Table 2: Model parameters

Symbol	Description	Value
$\boldsymbol{\beta}$	transmission probability per contact	0.03
τ	rate of treatment initiation among infected	0.1
N_0	initial population size	1000
$\hat{\boldsymbol{x}}$	proportion of system individuals by risk group	[0.05 0.20 0.75]
$\hat{\boldsymbol{e}}$	proportion of entering individuals risk by risk group	[0.05 0.20 0.75]
$\boldsymbol{\delta}$	average duration spent in each risk group	[5 15 25]
C	rate of contact formation among individuals in each risk group	[25 5 1]
ν	rate of population entry	0.05
μ	rate of population exit	0.03

All rates have units year^{-1}; durations are in years; parameters stratified by risk group are written [high, medium, low] risk.

entering the model by risk group $\hat{\boldsymbol{e}}$ were computed using the methods outlined in Appendix A.2.2, based on the following assumptions. First, we assumed that the proportion of individuals entering each risk group $\hat{\boldsymbol{e}}$ was equal to the proportion of individuals across risk groups in the model $\hat{\boldsymbol{x}}$. Second, we assumed that the average duration spent in each risk group $\boldsymbol{\delta}$ is known. Third, we assumed that the absolute number of individuals moving between two risk groups in either direction is balanced. These assumptions were chosen to avoid any dominant direction of turnover, so that the effects of turnover on model outputs would be attributable to movement of people between risk groups in general, rather than in one specific direction. The system of equations which results from these assumptions is given in Appendix B.2. To meet all three conditions, there is only one possible value for each element in ϕ and $\hat{\boldsymbol{e}}$. In other words, by specifying these three conditions, we ensure that a unique set of ϕ and $\hat{\boldsymbol{e}}$ is computed.

Using the above three assumptions, we need to specify the values of $\hat{\boldsymbol{x}}$, $\boldsymbol{\delta}$, ν, and μ. Such parameters could be derived from data as described in Section A.2.2; however, in this experiment, we use the illustrative values summarized in Table 2. After resolving the system of equations, $\hat{\boldsymbol{e}}$ is equal to $\hat{\boldsymbol{x}}$ (assumed), and ϕ is:

$$\phi = \begin{bmatrix} * & 0.0833 & 0.0867 \\ 0.0208 & * & 0.0158 \\ 0.0058 & 0.0042 & * \end{bmatrix} \tag{3}$$

We then simulated epidemics using these parameters. The model was initialized with $N_0 = 1000$ individuals who are distributed across risk groups according to $\hat{\boldsymbol{x}}$. We seeded the epidemic with one infectious individual in each risk group at $t = 0$. There were no treated individuals at the start of the epidemic, and

so all individuals except the 3 infectious individuals were susceptible. We numerically solved the system of ordinary differential equations in Python[1] using Euler's method with a time step of $dt = 0.1$ years. The full system of model equations is given in Appendix B.1. All comparative analyses are then conducted at equilibrium, defined as a steady state at 500 years with $< 1\%$ difference in incidence per year.

2.3. Experiments

The experiments used to examine the influence of risk group turnover on model outputs are as follows.

2.3.1. Experiment 1: Influence of turnover on equilibrium incidence and prevalence

Experiment 1 examined the influence of turnover on equilibrium incidence and prevalence, across each risk group and overall. Incidence was defined as λ_i from Eq. (2), and prevalence was defined as $\hat{\mathcal{I}}_i = \frac{\mathcal{I}_i}{\mathcal{X}_i}$. As in similar experiments (Zhang et al., 2012; Henry and Koopman, 2015), the rates of turnover were scaled by a single parameter. However, because the model had $G = 3$ risk groups, multiplying a set of base rates ϕ by a scalar factor would have resulted in changes to the relative population size of risk groups $\hat{\boldsymbol{x}}$. Thus, we controlled the rates of turnover using the duration of individuals in the high risk group δ_H, such that a shorter δ_H implied higher rates of turnover among all groups. The duration of individuals in the medium risk group δ_M was then defined as a value between δ_H and the maximum duration μ^{-1} which scaled with δ_H following: $\delta_M = \delta_H + \kappa\left(\mu^{-1} - \delta_H\right)$, with $\kappa = 0.3$. The duration of individuals in the low risk group δ_L similarly scaled with δ_H, but due to existing constraints, specification of δ_H and δ_M results in only one possible value of δ_L. In this way, each value of δ_H was used to define a unique set of turnover rates ϕ whose elements all scaled inversely with the duration in the high risk group δ_H. The value of δ_H was then varied from 33 to 3 years to examine the influence of different turnover rates. The resulting durations in each group are shown in Figure 3.

We plotted the STI prevalence versus turnover for each risk group, and explored mechanisms which explained the observed trends, including movement of individuals between risk groups, and incidence. We also plotted the STI prevalence ratios between each combination of risk groups, to help form a basis for understanding the results of Experiments 2 and 3.

2.3.2. Experiment 2: Inferred risk heterogeneity with vs without turnover

Next, we examined the influence of turnover on the parameter values inferred via model fitting. Specifically, we fit the model, with and without turnover, to: 20% infection prevalence among the high risk group, 8.75% among the medium risk group, 3% among the low risk group, and 5% overall. We fit the contact rates

[1] Code for all aspects of the project is available at: https://github.com/c-uhs/turnover

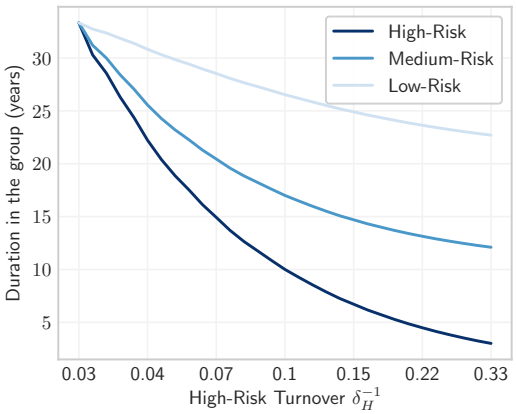

Figure 3: Average duration in each risk group as turnover rates vary.

C of all risk groups by minimizing the negative log-likelihood of each predicted prevalence versus the target.[2] We then compared the inferred contact rates C in the model with versus without turnover. The ratio of fitted (or posterior) contact rates C_H / C_L represents a measure of risk heterogeneity in the population, after fixing all other parameters, which produces the given infection prevalence.

2.3.3. Experiment 3: Influence of turnover on the TPAF of the highest risk group

Finally, Experiment 3 examined how the estimated contribution of highest risk group to overall transmission, as measured by the transmission population attributable fraction (TPAF), varied with versus without turnover. The TPAF of a risk group i is defined as:

$$\text{TPAF}_i(t) = \frac{I_0(t) - I_i(t)}{I_0(t)} \tag{4}$$

where $I_0(t)$ is the cumulative number of new infections by time t under usual conditions, and $I_i(t)$ is the cumulative number of new infections assuming no transmission from risk group i. Both $I_0(t)$ and $I_i(t)$ are calculated starting from a system at equilibrium.

We compared the two fitted models from Experiment 2, which were identical in structure except that one model had no turnover and one model had turnover (default parameterization described in Section 2.2). While prevalence was the same in both models, the group-specific contact rates inferred via model fitting were different. Following equilibration of both models, the TPAF of the high risk group was then estimated over a continuous time horizon.

[2] Sample sizes of 500, 2000, 7500, and 10,000 were assumed to generate binomial distributions for the high, medium, low, and overall prevalence targets respectively, and the minimization was performed using the SLSQP method (Kraft, 1988) from the SciPy Python package (`scipy.optimize.minimize`).

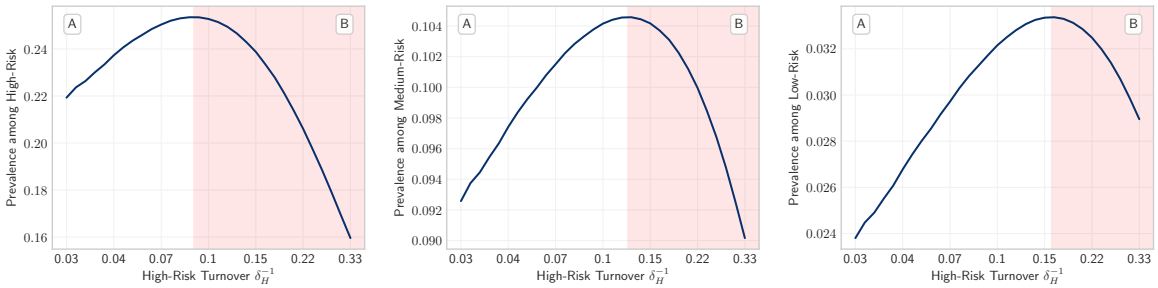

(a) High risk (b) Medium risk (c) Low risk

Figure 4: Equilibrium prevalence among high, medium, and low risk groups versus turnover, as controlled by the duration in the high risk group δ_H. Turnover shown in log scale.

3. Results

In this section we summarize the results of the experiments described in Section 2.3.

3.1. Experiment 1: How turnover influences equilibrium incidence and prevalence

Figure 4 illustrates trends in equilibrium STI prevalence among the high, medium, low, risk groups, versus turnover. In all three cases, the same profile was observed: at low turnover, increasing turnover increased prevalence, up to a maximum value (region A), and increasing turnover beyond this point (region B) then decreased equilibrium prevalence. In the highest risk group (Figure 4a), this transition occurred at a lower rate of turnover, while in the lowest risk group (Figure 4c), the transition occurred at a higher rate of turnover. This peaked prevalence profile can be explained by the interaction between two factors: the movement of individuals between risk groups, and incidence.

3.1.1. Movement of individuals between risk groups

The first factor, movement of individuals between risk groups, is illustrated in Figure 5 for four rates of turnover. We assumed that the distribution of health states among individuals leaving a risk group is equal to the distribution of health states within the group. Therefore, in the low risk group, a higher proportion of individuals leaving the group due to turnover were susceptible, as compared to individuals entering the group, who were more likely to be infectious. Thus, in the low risk group, turnover yielded a net replacement of susceptible individuals with infectious individuals. As a result, increasing turnover at low rates of turnover increased prevalence among the low risk group (Figure 4c, region A). Among the high risk group, turnover yielded a net replacement of both infectious and treated individuals with susceptible individuals. However, since incidence in the group was high, infection of new susceptible individuals from turnover outpaced the loss of infectious individuals via turnover for low rates of turnover. As a result, STI prevalence in the high risk group also increased with turnover for low rates of turnover (Figure 4a, region A). In order to explain the reversal of these trends in region B, the second factor, incidence, must be considered.

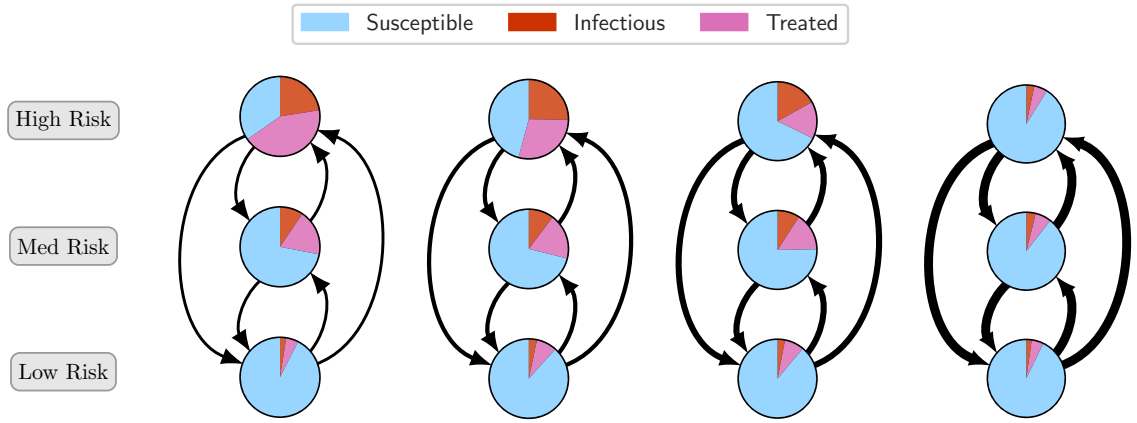

(a) Low turnover (b) Moderate turnover (c) High turnover (d) Very high turnover

Figure 5: Average health states of individuals moving between high and low risk groups due to different rates of turnover.

3.1.2. Incidence

As shown in Appendix B.4, incidence is proportional to two dynamic components: $\hat{C}_{\mathcal{I}}$ the average contact rate among infectious individuals, and $\hat{\mathcal{I}}$ overall prevalence.[3] Therefore, the influence of turnover on equilibrium incidence can be understood through the influence of turnover on these two components (Figure 6). Increasing turnover monotonically decreased the first component: $\hat{C}_{\mathcal{I}}$ the average contact rate among infectious individuals (Figure 6a), because turnover caused a net movement of infectious individuals from high to low risk. For low rates of turnover, however, turnover increased the second component: $\hat{\mathcal{I}}$ overall prevalence (Figure 6b, region A). For low rates of turnover, overall prevalence $\hat{\mathcal{I}}$ increased faster with turnover than the average contact rate of infectious people $\hat{C}_{\mathcal{I}}$ decreased. As a product of these two components, incidence then increased with turnover in region A (Figure 6c). The transition between regions A and B in Figure 6c (maximum equilibrium incidence) occurred when the dominating component between $\hat{\mathcal{I}}$ and $\hat{C}_{\mathcal{I}}$ reversed – that is, when the average contact rate of infectious people $\hat{C}_{\mathcal{I}}$ decreased with turnover faster than prevalence $\hat{\mathcal{I}}$ increased with turnover, causing incidence to decline. Then, as rates of turnover increased further, declining incidence also reduced prevalence, and incidence and prevalence decreased across all groups in mutually reinforcing decline. This mechanism explains the observations shown in region B throughout.

3.1.3. Prevalence ratios

Figure 7 shows the equilibrium prevalence ratios in comparisons of all three risk groups. The prevalence ratio between highest and lowest risk groups monotonically decreases with turnover (Figure 7a). Since

[3] Since we assumed proportionate mixing among risk groups, and only consider heterogeneity in contact rate C_i, incidence in each risk group is proportional to overall incidence with C_i as a scale factor (Figure C.1).

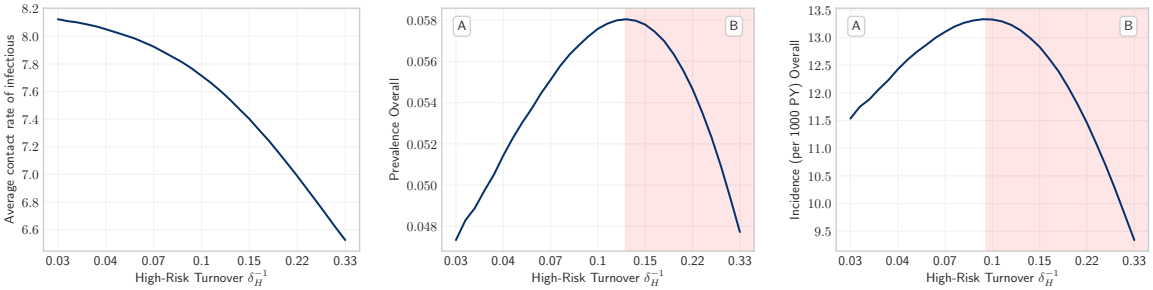

(a) Average contact rate among infectious individuals $\hat{C}_{\mathcal{I}}$

(b) Overall prevalence $\hat{\mathcal{I}}$

(c) Overall incidence λ

Figure 6: Incidence and the dynamic factors of incidence versus turnover. The product of components (a) and (b) is proportional to (c) overall incidence.

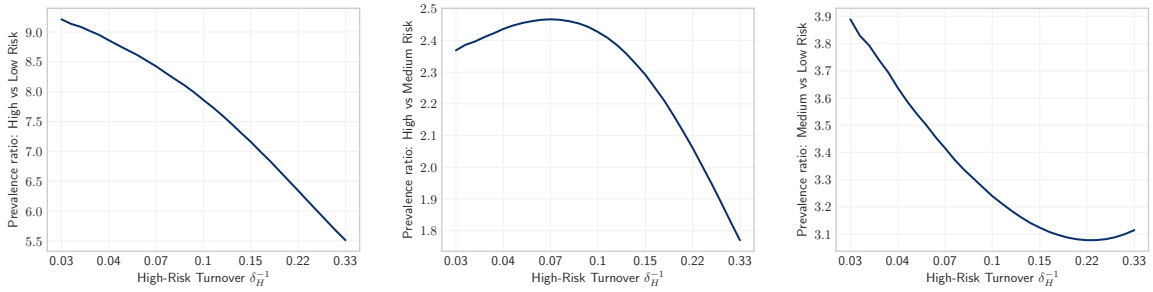

(a) High vs Low risk

(b) High vs Medium Risk

(c) Medium vs Low Risk

Figure 7: Equilibrium prevalence ratios between risk groups under different rates of turnover ϕ.

incidence ratios were not affected by turnover (Figure C.2), this decrease in prevalence ratio with turnover was attributed to the movement of individuals between risk groups, namely infectious individuals from high-to-low risk, and non-infectious individuals from low-to-high risk. This movement of individuals can also explain why prevalence among the high risk group can decrease with turnover, even as incidence increases (region B in Figure 4a overlaps region A in Figure 6c), while prevalence among the low risk group can increase with turnover, even as incidence decreases (region A in Figure 4c overlaps region B in Figure 6c). The high-to-medium and medium-to-low prevalence ratios are not monotonic, but for moderate rates of turnover, they follow the same trends as the high-to-low prevalence ratio. For low rates of turnover, the high-to-medium prevalence ratio (Figure 7b) increases slightly as prevalence among the high risk group increases with turnover faster than among the medium risk group. Similarly, for high rates of turnover, the medium-to-low prevalence ratio (Figure 7c) increases slightly as prevalence among the medium risk group declines faster with turnover than among the low risk group.

Table 3: Equilibrium contact rates and prevalence among the high and low risk groups predicted by the models with and without turnover, before and after model fitting.

	Contact Rate			Prevalence		
Context	High	Low	High/Low	High	Low	High/Low
No Turnover	25.0	1.0	25.0	21.9%	2.4%	**9.2**
Turnover	25.0	1.0	25.0	21.6%	3.2%	**6.7**
No Turnover [fit]	23.5	1.5	**15.2**	20.0%	3.0%	6.7
Turnover [fit]	24.3	1.0	**23.9**	20.0%	3.0%	6.7

3.2. Experiment 2: Inferred risk heterogeneity with vs without turnover

Next, we compared the fitted parameters in models with versus without turnover ($\delta_H = 5$ vs. $\delta_H = 33$ years). Before model fitting, the predicted prevalence ratio between high and low risk groups was lower with turnover than without: 6.7 vs 9.2. This reflects the "homogenizing" effect of turnover on the average risk experienced by individuals in the model. As shown in Figure 7a, the high-to-low prevalence ratio consistently declined with turnover. Thus, when fitting the model to target prevalence values, the fitted contact rates C would have to compensate for this difference in prevalence ratio with and without turnover.

After fitting the contact rates, both models predicted the target equilibrium infection prevalence values of 20%, 8.75%, 3%, and 5% among the high, medium, low risk groups, and overall (Figure C.3). However, in order to do so, the ratio of fitted contact rates between high and low risk groups (C_H / C_L) was higher with turnover than without: 23.9 vs 15.2 (Table 3). That is, the inferred level of risk heterogeneity was higher in the model with turnover than in the model without turnover. This is because, in order to observe the same prevalence ratio in a system with turnover, the "risk homogenizing" effects of turnover must be overcome by greater heterogeneity in risk, as compared to a system without turnover.

3.3. Experiment 3: Influence of turnover on the TPAF of the highest risk group

Finally, we compared the predicted TPAF of the highest risk group with and without turnover, after fitting to the same prevalence data (Figure 8). The TPAF approaches 1 for both models over the 50 year period, indicating that unmet treatment needs of the highest risk group are central to epidemic persistence in both scenarios. The estimated TPAF of the highest risk group is also higher in the model with turnover versus in the model without turnover over all time horizons. This increase in TPAF of the highest risk group can be attributed to a higher ratio of fitted contact rates C_H / C_L in the model with turnover is higher than in the model without (Experiment 2). The increased contact rate ratio affords a higher risk of onward transmission to the highest risk group in the model with turnover, and thus an increase in TPAF.

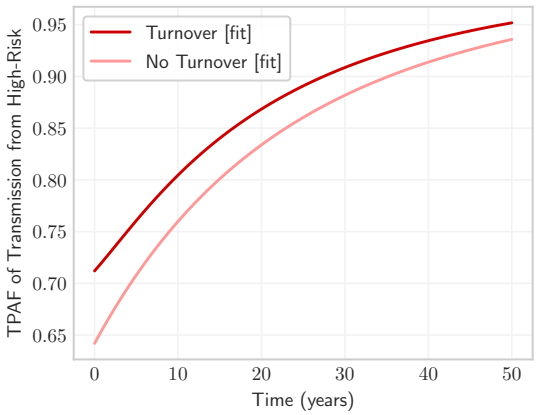

Figure 8: Transmission population attributable fraction (TPAF-from) of the high risk group in models with and without turnover, after fitting contact rates to group-specific prevalence.

This result then implies that models which fail to capture turnover dynamics which are present in reality may underestimate the TPAF of high risk groups.

4. Discussion

We developed a new framework for modelling turnover of individuals among risk groups, based on a flexible combination of data-driven constraints. We then used this framework to explore the influence of turnover on the contribution of the highest risk group to onward transmission in an illustrative STI epidemic without STI-attributable mortality. We found that failure to model turnover when simulating settings with turnover could result in underestimation of the contribution of the highest risk group to onward transmission.

Influence of turnover on incidence & prevalence. We found that turnover influences the overall equilibrium STI incidence and prevalence in a pattern consistent with previous works (Stigum et al., 1994; Zhang et al., 2012; Henry and Koopman, 2015). However, unlike previous works, we also illustrated the influence of turnover on group-specific prevalence, and demonstrated mechanistically how this occurs. For example, we showed that some infections among the low risk groups were acquired by individuals during a previous period of higher risk (see Appendix C.8 for additional results). We can summarize this influence of turnover, including reduced ratio of STI prevalence between the highest and lowest risk groups, as "reducing heterogeneity in risk" via movement of individuals between risk groups. Henry and Koopman (2015) demonstrated that such reduction in risk heterogeneity through turnover decreases the basic reproductive number and thus, means epidemic control could be easier to achieve. Our findings on the mechanisms by which increasing turnover reduces the STI treatment rate to achieve zero prevalence further supports these insights from Henry and Koopman (2015).

Implications for interventions. Our comparison of models with and without turnover, calibrated to the same epidemic, showed that if turnover exists in a given setting but it is ignored in a model, the TPAF of high risk groups will be underestimated by the model. This is because heterogeneity in risk must be higher in the presence of turnover than in a model without turnover in order to produce the same epidemic features. Although we examined a single parameter to capture risk (frequency of partner change), these insights would be generalizable to any other component of susceptibility or infectivity, because the risk per susceptible individual (force of infection) includes both biological transmission probabilities and frequency of partner change (Anderson and May, 1991). In the context of models with assortative mixing (individuals are more likely to form partnerships with other individuals in their risk group), the difference between the TPAFs estimated by the model with vs. without turnover is therefore expected to be even larger. The public health implication of models ignoring turnover which is present in reality is that the TPAF of high risk groups will be systematically underestimated, potentially misguiding resources away from high risk groups. Follow on research should quantify the size of this potential bias in TPAFs generated from models without turnover, and characterize the epidemiologic conditions under which the bias would be largest.

Turnover framework. The proposed framework provides a flexible way to parameterize risk group turnover based on available epidemiologic data and/or assumptions. The approach has four advantages. First, the framework defines how specific epidemiologic data and assumptions can be used as constraints to help define rates of turnover (Table 1). These data and assumptions are further discussed in the next paragraph. Second, the framework allows such constraints, which take the form $b_k = A_k\boldsymbol{\theta}$ to be chosen and combined in a flexible way, depending on which data are available, or which assumptions are most plausible. While it is necessary that constraints do not conflict one another, it is not necessary that a complete set of G^2 constraints be defined (where G is the number of risk groups), since optimization techniques can be used to calculate, for example, the smallest possible values of the parameters which satisfy the given constraints. Third, this flexible approach also allows the framework to scale to any number of risk groups, G. Fourth, we have shown how several previous implementations of turnover (Stigum et al., 1994; Eaton and Hallett, 2014; Henry and Koopman, 2015) can be recreated exactly using the proposed framework (Appendix A.3). In so doing, we highlight which specific assumptions are the same and which are different across the different implementations.

The major data needs of this approach include the following four categories. First, the proportion of total individuals in each risk group $\hat{x}_i$ is required. In the context of STIs, risk group size estimates may be obtained from demographic health surveys (USAID, 2019), and from mapping and enumeration of marginalized populations, such as sex workers (Abdul-Quader et al., 2014). For example, one risk group may be defined by any engagement in casual sex within the past year, and the corresponding proportion of the population could be estimated from self-reported behaviours in demographic health surveys (USAID, 2019).

Second, the proportion of individuals who enter into each risk group $\hat{e}_i$ upon entry into the model can be used to define additional constraints. Such proportions could be obtained the same way as $\hat{x}_i$ above, except using only data from individuals who recently became sexually active. For example, among women who became sexually active in the past year, what proportion also engaged in casual sex within the past year. If data on sexual debut is not available, then recent entry into sexual activity could be approximated using a suitable age range. Third, the average duration of time spent within each risk group δ_i can similarly be used to define additional constraints. Cross-sectional survey questions asked of female sex workers such as "for how many years have you been a sex worker?" may be used to obtain estimates of duration in sex work, with the recognition that such data are censured (Watts et al., 2010). Longitudinal, or cohort studies that track the self-reported sexual behaviour over time can also provide estimates of duration within variable periods of risk (Fergus et al., 2007). Fourth, similar studies may provide data on trajectories in risk behaviour of individuals over time, which can be used to estimates transition rates ϕ or ratios of transition rates. For example, upon retirement from sex work, a proportion of former sex workers may enter into monogamous relationships, while another proportion may continue to form multiple partnerships.

Limitations. There are six limitations of the study that are important when considering the proposed turnover framework and the implications of our results. First, our approach does not account for infection-attributable mortality, such as HIV-attributable mortality. It is well-established that HIV-attributable mortality will reduce the relative size of higher risk groups, and that alone can cause an epidemic to decline (Boily and Mâsse, 1997). As such, many models of HIV transmission that include very small ($< 3\%$ of the population) high risk groups, such as female sex workers, often do not constrain the relative size of the sub-group populations to be stable over time (Pickles et al., 2013). Second, we assumed a single-sex population and did not stratify by age. In the context of real-world STI epidemics, the relative size of risk groups may differ by both sex and age, such as the number of females who sell sex, versus the number of males who sell sex, versus the number of males who pay for sex (clients). Future work on the proposed framework could incorporate infection-attributable mortality, and age-sex stratifications into the model. Third, we assumed that turnover rates were not affected by the health status of individuals, which could change the observed influence of turnover on equilibrium STI incidence and prevalence. While changes to health state may affect the sexual behaviour of individuals, its not clear what overall patterns emerge at the population level. Fourth, we did not include individuals becoming re-susceptible – an important feature of many STIs such as syphilis and gonorrhoea (Fenton et al., 2008). As shown by Fenton et al. (2008) and Pourbohloul et al. (2003), the re-supply of susceptible individuals following STI treatment will fuel an epidemic, and so the influence of turnover on STI incidence, prevalence, and TPAF may be different, and warrants future study. Fifth, our analyses were restricted to equilibrium STI prevalence and incidence. The influence of turnover at different phases of an epidemic – growth, mature, declining – are expected to vary, and thus

represents an important topic for future investigation. Finally, our analyses reflected an illustrative STI epidemic in a population with illustrative risk strata. Future work should explore more realistic systems for specific STIs, such as the work by Johnson and Geffen (2016).

Conclusion. In conclusion, turnover in risk will influence epidemic model outputs, including projected incidence, prevalence, and measures of the contribution of high risk groups to overall STI transmission. Turnover should therefore be considered in transmission models with heterogeneity in risk. The methods presented here illustrate how epidemiologic data can be used to parametrize turnover in epidemic models. We hope that this will support accurate estimation of the importance of addressing the unmet needs of high risk populations – including gay men and other men who have sex with men, transgender women, people who use drugs, and people of all genders who sell sex – to achieve population-level transmission reduction.

Acknowledgements

We would like to thank Kristy Yiu (MAP Centre for Urban Health Solutions, Unity Health Toronto) for her logistical support, the Siyaphambili research team for helpful discussions, and Carly Comins (Johns Hopkins University) for facilitating the modelling meetings with the wider study team. SM is supported by an Ontario HIV Treatment Network and Canadian Institutes of Health Research New Investigator Award.

Contributions

JK and SM conceptualized the study, and drafted the manuscript; JK designed the experiments with input from LW, HM, and SM. JK developed the unified framework and conducted the modelling, experiments, and analyses and drafted the first version of the manuscript; All authors contributed to interpretation of the results and manuscript revision.

Funding

The study was supported by the National Institutes of Health, Grant number: NR016650; the Center for AIDS Research, Johns Hopkins University through the National Institutes of Health, Grant number: P30AI094189.

Conflicts of Interest

Declarations of interest: none.

References

Abu S Abdul-Quader, Andrew L Baughman, and Wolfgang Hladik. Estimating the size of key populations: Current status and future possibilities. 9(2):107–114, mar 2014. DOI 10.1097/COH.0000000000000041.

Roy M Anderson and Robert M May. Infectious diseases of humans: dynamics and control. *Infectious diseases of humans: dynamics and control.*, 1991.

Stefan Baral, Sosthenes Ketende, Jessie L. Green, Ping-An An Chen, Ashley Grosso, Bhekie Sithole, Cebisile Ntshangase, Eileen Yam, Deanna Kerrigan, Caitlin E. Kennedy, and Darrin Adams. Reconceptualizing the HIV epidemiology and prevention needs of female sex workers (FSW) in Swaziland. *PLoS ONE*, 9(12):e115465, dec 2014. DOI 10.1371/journal.pone.0115465.

Marie Claude Boily and Benoît Mâsse. Mathematical models of disease transmission: A precious tool for the study of sexually transmitted diseases. *Canadian Journal of Public Health*, 88(4):255–265, 1997. DOI 10.1007/bf03404793.

Marie Claude Boily, Michael Pickles, Michel Alary, Stefan Baral, James Blanchard, Stephen Moses, Peter Vickerman, and Sharmistha Mishra. What really is a concentrated HIV epidemic and what does it mean for West and Central Africa? Insights from mathematical modeling. *Journal of Acquired Immune Deficiency Syndromes*, 68:S74–S82, mar 2015. DOI 10.1097/QAI.0000000000000437.

Kelsey Case, Peter Ghys, Eleanor Gouws, Jeffery Eaton, Annick Borquez, John Stover, Paloma Cuchi, Laith Abu-Raddad, Geoffrey Garnett, and Timothy Hallett. Understanding the modes of tranmission model of new HIV infection and its use in prevention planning. *Bulletin of the World Health Organization*, 90(11):831–838, nov 2012. DOI 10.2471/blt.12.102574.

DataBank. Population estimates and projections, 2019. URL https://databank.worldbank.org/source/population-estimates-and-projections.

Jeffrey W. Eaton and Timothy B. Hallett. Why the proportion of transmission during early-stage HIV infection does not predict the long-term impact of treatment on HIV incidence. *Proceedings of the National Academy of Sciences*, 111(45): 16202–16207, nov 2014. DOI 10.1073/pnas.1323007111.

Kevin A. Fenton, Romulus Breban, Raffaele Vardavas, Justin T. Okano, Tara Martin, Sevgi Aral, and Sally Blower. Infectious syphilis in high-income settings in the 21st century. *The Lancet Infectious Diseases*, 8(4):244–253, apr 2008. DOI 10.1016/S1473-3099(08)70065-3.

Stevenson Fergus, Marc A Zimmerman, and Cleopatra H Caldwell. Growth trajectories of sexual risk behavior in adolescence and young adulthood. *American Journal of Public Health*, 97(6):1096–1101, jun 2007. DOI 10.2105/AJPH.2005.074609.

Geoffrey P. Garnett and Roy M. Anderson. Balancing sexual partnership in an age and activity stratified model of HIV transmission in heterosexual populations. *Mathematical Medicine and Biology*, 11(3):161–192, jan 1994. DOI 10.1093/imammb/11.3.161.

Christopher J. Henry and James S. Koopman. Strong influence of behavioral dynamics on the ability of testing and treating HIV to stop transmission. *Scientific Reports*, 5(1):9467, aug 2015. DOI 10.1038/srep09467.

ICAP. PHIA Project, 2019. URL https://phia.icap.columbia.edu.

Leigh F. Johnson and Nathan Geffen. A Comparison of two mathematical modeling frameworks for evaluating sexually transmitted infection epidemiology. *Sexually Transmitted Diseases*, 43(3):139–146, mar 2016. DOI 10.1097/OLQ.0000000000000412.

J S Koopman, J A Jacquez, G W Welch, C P Simon, B Foxman, S M Pollock, D Barth-Jones, A L Adams, and K Lange. The role of early HIV infection in the spread of HIV through populations. *Journal of Acquired Immune Deficiency Syndromes*, 14(3):249–58, mar 1997. URL http://www.ncbi.nlm.nih.gov/pubmed/9117458.

Dieter Kraft. A software package for sequential quadratic programming. Technical Report DFVLR-FB 88-28, DLR German Aerospace Center — Institute for Flight Mechanics, Koln, Germany, 1988.

LAPACK. LAPACK: Linear Algebra PACKage, 1992. URL http://www.netlib.org/lapack.

Charles L Lawson and Richard J Hanson. *Solving least squares problems*, volume 15. SIAM, 1995.

Thomas Robert Malthus. *An Essay on the Principle of Population*. 1798.

Cicely Marston and Eleanor King. Factors that shape young people's sexual behaviour: a systematic review. *Lancet*, 368 (9547):1581–1586, nov 2006. DOI 10.1016/S0140-6736(06)69662-1.

Sharmistha Mishra, Richard Steen, Antonio Gerbase, Ying Ru Lo, and Marie Claude Boily. Impact of High-Risk Sex and Focused Interventions in Heterosexual HIV Epidemics: A Systematic Review of Mathematical Models. *PLoS ONE*, 7(11): e50691, nov 2012. DOI 10.1371/journal.pone.0050691.

Sharmistha Mishra, Michael Pickles, James F Blanchard, Stephen Moses, and Marie Claude Boily. Distinguishing sources of HIV transmission from the distribution of newly acquired HIV infections: Why is it important for HIV prevention planning? *Sexually Transmitted Infections*, 90(1):19–25, feb 2014. DOI 10.1136/sextrans-2013-051250.

Sharmistha Mishra, Marie-Claude Boily, Sheree Schwartz, Chris Beyrer, James F. Blanchard, Stephen Moses, Delivette Castor, Nancy Phaswana-Mafuya, Peter Vickerman, Fatou Drame, Michel Alary, and Stefan D. Baral. Data and methods to characterize the role of sex work and to inform sex work programs in generalized HIV epidemics: evidence to challenge assumptions. *Annals of Epidemiology*, 26(8):557–569, aug 2016. DOI 10.1016/j.annepidem.2016.06.004.

Christinah Mukandavire, Josephine Walker, Sheree Schwartz, Marie-Claude Boily, Leon Danon, Carrie Lyons, Daouda Diouf, Ben Liestman, Nafissatou Leye Diouf, Fatou Drame, Karleen Coly, Remy Serge Manzi Muhire, Safiatou Thiam, Papa Amadou Niang Diallo, Coumba Toure Kane, Cheikh Ndour, Erik Volz, Sharmistha Mishra, Stefan Baral, and Peter Vickerman. Estimating the contribution of key populations towards the spread of HIV in Dakar, Senegal. *Journal of the International AIDS Society*, 21:e25126, jul 2018. DOI 10.1002/jia2.25126.

Michael Pickles, Marie Claude Boily, Peter Vickerman, Catherine M Lowndes, Stephen Moses, James F Blanchard, Kathleen N Deering, Janet Bradley, Banadakoppa M Ramesh, Reynold Washington, Rajatashuvra Adhikary, Mandar Mainkar, Ramesh S Paranjape, and Michel Alary. Assessment of the population-level effectiveness of the Avahan HIV-prevention programme in South India: A preplanned, causal-pathway-based modelling analysis. *The Lancet Global Health*, 1(5):e289–e299, nov 2013. DOI 10.1016/S2214-109X(13)70083-4.

Babak Pourbohloul, Michael L. Rekart, and Robert C. Brunham. Impact of mass treatment on syphilis transmission: A mathematical modeling approach. *Sexually Transmitted Diseases*, 30(4):297–305, apr 2003. DOI 10.1097/00007435-200304000-00005.

Zara Shubber, Sharmistha Mishra, Juan F. Vesga, and Marie Claude Boily. The HIV modes of transmission model: A systematic review of its findings and adherence to guidelines. *Journal of the International AIDS Society*, 17(1):18928, jan 2014. DOI 10.7448/IAS.17.1.18928.

Hein Stigum, W. Falck, and P. Magnus. The core group revisited: The effect of partner mixing and migration on the spread of gonorrhea, chlamydia, and HIV. *Mathematical Biosciences*, 120(1):1–23, mar 1994. DOI 10.1016/0025-5564(94)90036-1.

USAID. The DHS Program, 2019. URL https://www.dhsprogram.com.

C. Watts, C. Zimmerman, A. M. Foss, M. Hossain, A. Cox, and P. Vickerman. Remodelling core group theory: the role of sustaining populations in HIV transmission. *Sexually Transmitted Infections*, 86(Suppl 3):iii85–iii92, dec 2010. DOI 10.1136/sti.2010.044602.

James A Yorke, Herbert W Hethcote, and Annett Nold. Dynamics and control of the transmission of gonorrhea. *Sexually Transmitted Diseases*, 5(2):51–56, 1978. DOI 10.1097/00007435-197804000-00003.

Xinyu Zhang, Lin Zhong, Ethan Romero-Severson, Shah Jamal Alam, Christopher J Henry, Erik M Volz, and James S Koopman. Episodic HIV Risk Behavior Can Greatly Amplify HIV Prevalence and the Fraction of Transmissions from Acute HIV Infection. *Statistical Communications in Infectious Diseases*, 4(1), nov 2012. DOI 10.1515/1948-4690.1041.

A. Turnover System

We introduce a system of parameters and constraints to describe risk group turnover in deterministic epidemic models with heterogeneity in risk. We then describe how the system can be used in practical terms, based on different assumptions and data available for parameterizing turnover in risk. We conclude by framing previous approaches to this task using the proposed system.

A.1. Notation

Consider a population divided into G risk groups. We denote the number of individuals in risk group $i \in [1, \ldots, G]$ as x_i and the set of all risk groups as $\boldsymbol{x} = \{x_1, \ldots, x_G\}$. The total population size is $N = \sum_i x_i$, and the relative population size of each group is denoted as $\hat{x}_i = x_i/N$. Individuals enter the population at a rate ν per year, and exit at a rate μ per year. We model the distribution of risk groups among individuals entering into the population as $\hat{\boldsymbol{e}}$, which may be different from individuals already in the population $\hat{\boldsymbol{x}}$.[4] Thus, the total number of individuals entering into population $\boldsymbol{x}$ per year is given by νN, and the number of individuals entering into group x_i specifically is given by $\hat{e}_i \nu N$.

Turnover transitions may then occur between any two groups, in either direction. Therefore we denote the turnover rates as a $G \times G$ matrix ϕ. The element ϕ_{ij} corresponds to the proportion of individuals in group x_i who move from group x_i to group x_j each year. An example matrix is given in Eq. (A.1), where we write the diagonal elements as $*$ since they represent transitions from a group to itself.

$$\phi = \begin{bmatrix} * & x_1 \to x_2 & \cdots & x_1 \to x_G \\ x_2 \to x_1 & * & \cdots & x_2 \to x_G \\ \vdots & \vdots & \ddots & \vdots \\ x_G \to x_1 & x_G \to x_2 & \cdots & * \end{bmatrix} \tag{A.1}$$

Risk groups, transitions, and the associated rates are also shown for $G = 3$ in Figure A.1.

A.2. Parameterization

Next, we construct a system like the one above which reflects the risk group dynamics observed in a specific context. We assume that the relative sizes of the risk groups in the model ($\hat{\boldsymbol{x}}$) are already known, and should remain constant over time. Thus, what remains is to estimate the values of the parameters: ν, μ, $\hat{\boldsymbol{e}}$, and ϕ, using commonly available sources of data.

[4] We could equivalently stratify the rate of entry ν by risk group; however, we find that the mathematics in subsequent sections are more straightforward using $\hat{\boldsymbol{e}}$.

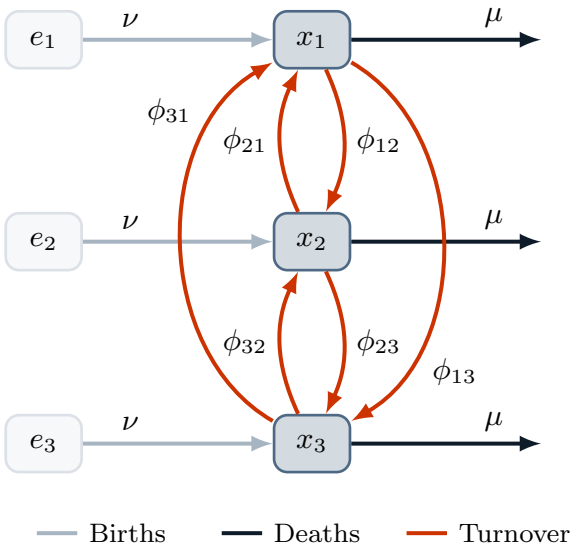

Figure A.1: System of risk groups and flows between them for $G = 3$

A.2.1. Total Population Size

The total population size $N(t)$ is a function of the rates of population entry $\nu(t)$ and exit $\mu(t)$, given an initial size N_0. We allow the proportion entering the system to vary by risk group via $\hat{\boldsymbol{e}}$, while the exit rate has the same value for each group. We assume that there is no disease-attributable death. Because the values of ν and μ are the same for each risk group, they can be estimated independent of $\hat{\boldsymbol{x}}$, $\hat{\boldsymbol{e}}$, and ϕ.

The difference between entry and exit rates defines the rate of population growth:

$$\mathcal{G}(t) = \nu(t) - \mu(t) \tag{A.2}$$

The total population may then be defined using an initial population size N_0 as:

$$N(t) = N_0 \exp\left(\int_0^t \log\left(1 + \mathcal{G}(\tau)\right) d\tau\right) \tag{A.3}$$

which, for constant growth, simplifies to the familiar expression (Malthus, 1798):

$$N(t) = N_0(1 + \mathcal{G})^t \tag{A.4}$$

Census data, such as (DataBank, 2019), can be used to source the total population size in a given geographic setting over time $N(t)$, thus allowing Eqs. (A.3) and (A.4) to be used to estimate $\mathcal{G}(t)$.

If the population size is assumed to be constant, then $\mathcal{G}(t) = 0$ and $\nu(t) = \mu(t)$. If population growth occurs at a stable rate, then $\mathcal{G}$ is fixed at a constant value which can be estimated via Eq. (A.4) using any two values of $N(t)$, separated by a time interval τ:

$$\mathcal{G}_\tau = \frac{N(t+\tau)^{\frac{1}{\tau}}}{N(t)} - 1 \tag{A.5}$$

If the rate of population growth $\mathcal{G}$ varies over time, then Eq. (A.5) can be reused for consecutive time intervals, and the complete function $\mathcal{G}(t)$ approximated piecewise by constant values. The piecewise approximation can be more feasible than exact solutions using Eq. (A.3), and can reproduce $N(t)$ accurately for small enough intervals τ, such as one year.

Now, given a value of $\mathcal{G}(t)$, either $\nu(t)$ must be chosen and $\mu(t)$ calculated using Eq. (A.2), or $\mu(t)$ must be chosen, and $\nu(t)$ calculated. Most modelled systems assume a constant duration of time that individuals spend in the model $\delta(t)$ (Anderson and May, 1991) which is related to the rate of exit μ by:

$$\delta(t) = \mu^{-1}(t) \tag{A.6}$$

In the context of sexually transmitted infections, the duration of time usually reflects the average sexual life-course of individuals from age 15 to 50 years, such that $\delta = 35$ years. The duration δ may also vary with time to reflect changes in life expectancy. The exit rate $\mu(t)$ can then be defined as $\delta^{-t}(t)$ following Eq. (A.6), and the entry rate $\nu(t)$ defined as $\mathcal{G}(t) - \mu(t)$ following Eq. (A.2).

A.2.2. Turnover

Next, we present methods for resolving the distribution of individuals entering the risk model $\hat{\boldsymbol{e}}(t)$ and the rates of turnover $\phi(t)$, assuming that entry and exit rates $\nu(t)$ and $\mu(t)$ are known. Similar to above, we first formulate the problem as a system of equations. Then, we explore the data and assumptions required to solve for the values of parameters in the system. The (t) notation is omitted throughout this section for clarity, though time-varying parameters can be estimated by repeating the necessary calculations for each t.

The number of risk groups G dictates the number of unknown elements in $\hat{\boldsymbol{e}}$ and ϕ: G and $G(G-1)$, respectively. We collect these unknowns in the vector $\boldsymbol{\theta} = [\hat{\boldsymbol{e}}, \boldsymbol{y}]$, where $\boldsymbol{y} = \text{vec}_{i \neq j}(\phi)$. For example, for $G = 3$, the vector $\boldsymbol{\theta}$ is defined as:

$$\boldsymbol{\theta} = \begin{bmatrix} \hat{e}_1 & \hat{e}_2 & \hat{e}_3 & \phi_{12} & \phi_{13} & \phi_{21} & \phi_{23} & \phi_{31} & \phi_{32} \end{bmatrix} \tag{A.7}$$

We then define a linear system of equations which uniquely determine the elements of $\boldsymbol{\theta}$:

$$\boldsymbol{b} = A\,\boldsymbol{\theta} \tag{A.8}$$

where A is a $M \times G^2$ matrix and $\boldsymbol{b}$ is a M-length vector. Specifically, each row in A and $\boldsymbol{b}$ defines a constraint: an assumed mathematical relationship involving one or more elements of $\hat{\boldsymbol{e}}$ and ϕ. For example, a simple constraint could be to assume the value $\hat{e}_2 = 0.20$. Each of the following sections introduces a type of constraint, including: assuming a constant group size, specifying elements of $\boldsymbol{\theta}$ directly, assuming an average duration in a group, and assuming relative rates of turnover. Constraints may be selected and combined together based on availability of data and plausibility of assumptions. However, a total of $M = G^2$ constraints must be defined in order to obtain a "unique solution": exactly one value of $\boldsymbol{\theta}$ which satisfies all

constraints. The values of $\hat{\boldsymbol{e}}$ and ϕ can then be calculated algebraically by solving Eq. (A.8) with $\boldsymbol{\theta} = A^{-1}\boldsymbol{b}$, for which many algorithms exist (LAPACK, 1992).

1. Constant group size. One epidemiologic feature that epidemic models consider is whether or not the relative sizes of risk groups are constant over time (Henry and Koopman, 2015; Boily et al., 2015). Assuming constant group size implies a stable level of heterogeneity over time. To enforce this assumption, we define the "conservation of mass" equation for group x_i, wherein the rate of change of the group is defined as the sum of flows in / out of the group:

$$\frac{d}{dt}x_i = \nu N\hat{e}_i + \sum_j \phi_{ji}\, x_j - \mu\, x_i - \sum_j \phi_{ij}\, x_i \tag{A.9}$$

Eq. (A.9) is written in terms of absolute population sizes $\boldsymbol{x}$, but can be written as proportions $\hat{\boldsymbol{x}}$ by dividing all terms by N. If we assume that the proportion of each group $\hat{x}_i$ is constant over time, then the desired rate of change for risk group i will be equal to the rate of population growth of the risk group, $\mathcal{G}x_i$. Substituting $\frac{d}{dt}x_i = \mathcal{G}x_i$ into Eq. (A.9), and simplifying yields:

$$\nu\, x_i = \nu\, N\hat{e}_i + \sum_j \phi_{ji}\, x_j - \sum_j \phi_{ij}\, x_i \tag{A.10}$$

Factoring the left and right hand sides in terms of $\hat{\boldsymbol{e}}$ and ϕ, we obtain G unique constraints. For $G = 3$, this yields the following 3 rows as the basis of $\boldsymbol{b}$ and A:

$$\boldsymbol{b} = \begin{bmatrix} \nu x_1 \\ \nu x_2 \\ \nu x_3 \end{bmatrix}; \qquad A = \begin{bmatrix} \nu & \cdot & \cdot & -x_1 & -x_1 & x_2 & \cdot & x_3 & \cdot \\ \cdot & \nu & \cdot & x_1 & \cdot & -x_2 & -x_2 & \cdot & x_3 \\ \cdot & \cdot & \nu & \cdot & x_1 & \cdot & x_2 & -x_3 & -x_3 \end{bmatrix} \tag{A.11}$$

These G constraints ensure risk groups do not change size over time. However, a unique solution requires an additional $G(G-1)$ constraints. For $G = 3$, this corresponds to 6 additional constraints.

2. Specified elements. The simplest type of additional constraint is to directly specify the values of individual elements in $\hat{\boldsymbol{e}}$ or ϕ. Such constraints may be appended to $\boldsymbol{b}$ and A as an additional row k using indicator notation.[5] That is, with b_k as the specified value v, and A_k as the indicator vector, with 1 in the same position as the desired element in $\boldsymbol{\theta}$:

$$b_k = v; \qquad A_k = [0, \ldots, 1, \ldots, 0] \tag{A.12}$$

For example, for $G = 3$, if it is known that 20% of individuals enter directly into risk group x_2 upon entry into the model ($\hat{e}_2 = 0.20$), then $\boldsymbol{b}$ and A can be augmented with:

$$b_k = \begin{bmatrix} 0.20 \end{bmatrix}; \qquad A_k = \begin{bmatrix} \cdot & 1 & \cdot & \cdot & \cdot & \cdot & \cdot & \cdot & \cdot \end{bmatrix} \tag{A.13}$$

[5] Indicator notation, also known as "one-hot notation" is used to select one element from another vector, based on its position. An indicator vector is 1 in the same location as the element of interest, and 0 everywhere else.

since $\hat{e}_2$ is the second element in $\boldsymbol{\theta}$. If the data suggest zero turnover from group i to group j, then Eq. (A.13) can also be used to set $\phi_{ij} = 0$.

Note that the elements of $\hat{\boldsymbol{e}}$ must sum to one. Therefore, specifying all elements in $\hat{\boldsymbol{e}}$ will only provide $G - 1$ constraints, as the last element will be either redundant or violate the sum-to-one rule. As shown in Appendix B.3, the sum-to-one rule is actually implicit in Eq. (A.11), so it is not necessary to supply a constraint like $1 = \sum_i \hat{e}_i$.

3. Group duration. Type 1 Constraints assume that the relative population size of each group remains constant. Another epidemiologic feature that epidemic models considered is whether or not the duration of time spent within a given risk group remains constant. For example, in STI transmission models that include formal sex work, it can be assumed that the duration in formal sex work work remains stable over time, such as in (Mishra et al., 2014; Boily et al., 2015). The duration δ_i is defined as the inverse of all rates of exit from the group:

$$\delta_i = \left(\mu + \sum_j \phi_{ij} \right)^{-1} \tag{A.14}$$

Estimates of the duration in a given group can be sourced from cross-sectional survey data where participants are asked about how long they have engaged in a particular practice – such as sex in exchange for money (Watts et al., 2010). Data on duration may also be sourced from longitudinal data, where repeated measures of self-reported sexual behaviour, or proxy measures of sexual risk data, are collected (USAID, 2019; ICAP, 2019). Data on duration in each risk group can then be used to define ϕ by rearranging Eq. (A.14) to yield: ${\delta_i}^{-1} - \mu = \sum_j \phi_{ij}$. For example, if for $G = 3$, the average duration in group x_1 is known to be $\delta_1 = 5$ years, then $\boldsymbol{b}$ and A can be augmented with another row k:

$$b_k = \begin{bmatrix} 5^{-1} - \mu \end{bmatrix}; \qquad A_k = \begin{bmatrix} \cdot & \cdot & \cdot & 1 & 1 & \cdot & \cdot & \cdot & \cdot \end{bmatrix} \tag{A.15}$$

Note that, similar to specifying all elements of $\hat{\boldsymbol{e}}$, specifying δ_i may result in conflicts or redundancies with other constraints. A conflict means it will not be possible to resolve values of ϕ which simultaneously satisfy all constraints, while a redundancy means that adding one constraint does not help resolve a unique set of values $\boldsymbol{\theta}$. For example, for $G = 3$, if Type 2 Constraints are used to specify $\phi_{12} = 0.1$ and $\phi_{13} = 0.1$, and $\mu = 0.05$, then by Eq. (A.14), we must have $\delta_1 = 4$. Specifying any other value for δ_1 will result in a conflict, while specifying $\delta_1 = 4$ is redundant, since it is already implied. There are innumerable situations in which this may occur, so we do not attempt to describe them all. Section A.2.2 describes how to identify conflicts and redundancies when they are not obvious.

4. Turnover rate ratios. In many cases, it may be difficult to obtain estimates of a given turnover rate ϕ_{ij} for use in Type 2 Constraints. However, it may be possible to estimate relative relationships between rates of turnover, such as:

$$r\,\phi_{ij} = \phi_{i'j'} \tag{A.16}$$

where r is a ratio relating the values of ϕ_{ij} and $\phi_{i'j'}$. For example, for $G = 3$, let T_1 be the total number of individuals entering group x_1 due to turnover. If we know that 70% of T_1 originates from group x_2, while 30% of T_1 originates from group x_3, then $0.7\,T_1 = \phi_{23}\,x_2$ and $0.3\,T_1 = \phi_{13}\,x_1$, and thus: $\phi_{23}\left(\frac{0.3\,x_2}{0.7\,x_1}\right) = \phi_{13}$. This constraint can then be appended as another row k in $\boldsymbol{b}$ and A like:

$$b_k = \begin{bmatrix} 0 \end{bmatrix}; \qquad A_k = \begin{bmatrix} \cdot & \cdot & \cdot & \cdot & \left(\frac{0.3\,x_2}{0.7\,x_1}\right) & \cdot & 1 & \cdot & \cdot \end{bmatrix} \tag{A.17}$$

The example in Eq. (A.17) is based on what proportions of individuals entering a risk group j came from which former risk group i, but similar constraints may be defined based on what proportions of individuals exiting a risk group i enter into which new risk group j. It can also be assumed that the absolute number of individuals moving between two risk groups is equal, in which case the relationship is: $\phi_{ij}\left(\frac{x_i}{x_j}\right) = \phi_{ji}$. All constraints of this type will have $b_k = 0$.

Solving the System. Table A.1 summarizes the four types of constraints described above. Given a set of sufficient constraints on $\boldsymbol{\theta}$ to ensure exactly one solution, the system of equations Eq. (A.8) can be solved using $\boldsymbol{\theta} = A^{-1}\boldsymbol{b}$. The resulting values of $\hat{\boldsymbol{e}}$ and ϕ can then be used in the epidemic model.

However, we may find that we have an insufficient number of constraints, implying that there are multiple values of the vector $\boldsymbol{\theta}$ which satisfy the constraints. An insufficient number of constraints may be identified by a "rank deficiency" warning in numerical solvers of Eq. (A.8) (LAPACK, 1992). Even if A has G^2 rows, the system may have an insufficient number of constraints because some constraints are redundant. In this situation, we can pose the problem as a minimization problem, namely:

$$\boldsymbol{\theta}^* = \arg\min f(\boldsymbol{\theta}), \quad \text{subject to: } \boldsymbol{b} = A\,\boldsymbol{\theta};\ \ \boldsymbol{\theta} \geq 0 \tag{A.18}$$

where f is a function which penalizes certain values of $\boldsymbol{\theta}$. For example, $f = ||\cdot||_2$ penalizes large values in $\boldsymbol{\theta}$, so that the smallest values of $\hat{\boldsymbol{e}}$ and ϕ which satisfy the constraints will be resolved.[6]

Similarly, we may find that no solution exists for the given constraints, since two or more constraints are in conflict. Conflicting constraints may be identified by a non-zero error in the solution to Eq. (A.8) (LAPACK, 1992). In this case, the conflict should be resolved by changing or removing one of the conflicting constraints.

A.3. Previous Approaches

Few epidemic models of sexually transmitted infections with heterogeneity in risk have simulated turnover among risk groups, and those models which have simulated turnover have done so in various ways. In this

[6] Numerical solutions to such problems are widely available, such as the Non-Negative Lease Squares solver (Lawson and Hanson, 1995), available in Python: `https://docs.scipy.org/doc/scipy/reference/generated/scipy.optimize.nnls.html`.

Table A.1: Summary of constraint types for defining risk group turnover

Name	Eq.	E.g.	Data requirements
1. Constant group size	(A.10)	(A.11)	all values of $\hat{x}_i$ and ν
2. Specified elements	(A.12)	(A.13)	any value of $\hat{e}_i$ or ϕ_{ij}
3. Group duration	(A.14)	(A.15)	any value of δ_i
4. Turnover rate ratios	(A.16)	(A.17)	any relationship between two turnover rates ϕ_{ij} and $\phi_{i'j'}$

ν: rate of population entry; ϕ_{ij}: rate of turnover from group i to group j; $\hat{x}_i$: proportion of individuals in risk group i; $\hat{e}_i$: proportion of individuals entering into risk group i; δ_i: average duration spent in risk group i.

section, we review three prior implementations of turnover and each study's objectives for the implementation – e.g. constant relative group sizes over time. We then highlight how the approach proposed in Section A.2 could be used to achieve the same objectives.

Stigum et al. (1994) simulated turnover among $G = 2$ risk groups in a population with no exogenous entry or exit ($\nu = \mu = 0$ and hence $\hat{\boldsymbol{e}}$ is not applicable). Turnover between the groups was balanced in order to maintain constant risk group sizes (Type 1 Constraint),[7] while the rate of turnover from high to low was specified as κ (Type 2 Constraint). Thus, the turnover system used by Stigum et al. (1994) can be written in the proposed framework as:

$$\begin{bmatrix} 0 \\ \kappa \end{bmatrix} = \begin{bmatrix} \hat{x}_1 & -\hat{x}_2 \\ 1 & \cdot \end{bmatrix} \begin{bmatrix} \phi_{12} \\ \phi_{21} \end{bmatrix}, \qquad \hat{e}_1 = \hat{e}_2 = 0 \tag{A.19}$$

Henry and Koopman (2015) also simulated turnover among $G = 2$ risk groups, but considered exogenous entry and exit, both at a rate μ. The authors used the notation f_i for our $\hat{x}_i$, and assumed that the exogenous population had the same distribution of risk groups as the system population: $\hat{e}_i = f_i$ (Type 2 Constraint). The authors further maintained constant risk group sizes (Type 1 Constraint) by analytically balancing turnover between the two groups using: $\phi_{12} = \omega\hat{x}_2$; $\phi_{21} = \omega\hat{x}_1$. However, it can be shown that this analytical approach is also the solution to the following combination of Type 1 and 2 Constraints:

$$\begin{bmatrix} 0 \\ \omega f_2 \end{bmatrix} = \begin{bmatrix} f_1 & -f_2 \\ 1 & \cdot \end{bmatrix} \begin{bmatrix} \phi_{12} \\ \phi_{21} \end{bmatrix}, \qquad \hat{e}_i = f_i \tag{A.20}$$

Eaton and Hallett (2014) simulated turnover among $G = 3$ risk groups, considering exogenous entry from a population with a unique distribution of risk groups $\hat{\boldsymbol{e}}$. Turnover was considered from high-to-medium, high-to-low, and medium-to-low risk, all with an equal rate ψ; the reverse transition rates were set to zero

[7] Due to its simplicity, this constraint is actually an example of both Type 1 and Type 4 Constraints.

(six total Type 2 Constraints). In the absence of turnover in the other direction, risk group sizes were maintained using the values of $\hat{e}_i$, computed using Type 1 Constraints as follows:

$$\begin{bmatrix} \nu x_1 + 2x_1\psi \\ \nu x_2 - x_1\psi + x_2\psi \\ \nu x_3 - x_1\psi - x_2\psi \end{bmatrix} = \begin{bmatrix} \nu & \cdot & \cdot \\ \cdot & \nu & \cdot \\ \cdot & \cdot & \nu \end{bmatrix} \begin{bmatrix} e_1 \\ e_2 \\ e_3 \end{bmatrix}, \qquad \begin{aligned} \phi_{12} = \phi_{13} = \phi_{23} = \psi \\ \phi_{21} = \phi_{31} = \phi_{32} = 0 \end{aligned} \tag{A.21}$$

In sum, the framework for modelling turnover presented in this section aims to generalize all previous implementations. In so doing, we hope to clarify the requisite assumptions, dependencies on epidemiologic data, and relationships between previous approaches.

B. Supplemental Equations

Table B.1: Notation

Symbol	Definition
i	risk group index
j	risk group index for "other" group in turnover
k	risk group index for "other" group in incidence
$\mathcal{S}_i$	Number of susceptible individuals in risk group i
$\mathcal{I}_i$	Number of infectious individuals in risk group i
$\mathcal{T}_i$	Number of treated individuals in risk group i
N	total population size
ν	rate of population entry
μ	rate of population exit
ϕ_{ij}	rate of turnover from group i to group j
λ_i	force of infection among susceptibles in risk group i
τ	rate of treatment initiation among infected
$\hat{x}_i$	proportion of individuals in risk group i
$\hat{e}_i$	proportion of individuals entering into risk group i
δ_i	average duration spent in risk group i
C_i	contact rate among individuals in risk group i
β	probability of transmission per contact
ρ_{ik}	probability of contact formation between risk groups i and k

B.1. Model Equations

$$\frac{d}{dt}\mathcal{S}_i(t) = \sum_j \phi_{ji}\mathcal{S}_j(t) - \sum_j \phi_{ij}\mathcal{S}_i(t) - \mu\mathcal{S}_i(t) + \nu\hat{e}_i N(t) - \lambda_i(t)\mathcal{S}_i(t) \tag{B.1}$$

$$\frac{d}{dt}\mathcal{I}_i(t) = \sum_j \phi_{ji}\mathcal{I}_j(t) - \sum_j \phi_{ij}\mathcal{I}_i(t) - \mu\mathcal{I}_i(t) + \lambda_i(t)\mathcal{S}_i(t) - \tau\mathcal{I}_i(t) \tag{B.2}$$

$$\frac{d}{dt}\mathcal{T}_i(t) = \sum_j \phi_{ji}\mathcal{T}_j(t) - \sum_j \phi_{ij}\mathcal{T}_i(t) - \mu\mathcal{T}_i(t) + \tau\mathcal{I}_i(t) \tag{B.3}$$

B.2. Complete Example Turnover System

$$
\begin{array}{r}
\text{constant group size} \\ \\ \\
\text{specified } e \\ \\ \\
\text{group duration} \\ \\ \\
\text{turnover rate ratios} \\ \\ \\
\end{array}
\left\{
\begin{array}{c}
\left[\begin{array}{c}
\nu x_1 \\ \nu x_2 \\ \nu x_3 \\ e_1^* \\ e_2^* \\ e_3^* \\ {\delta_1}^{-1} - \mu \\ {\delta_2}^{-1} - \mu \\ {\delta_3}^{-1} - \mu \\ 0 \\ 0 \\ 0
\end{array}\right]
\end{array}
\right.
=
\left[\begin{array}{ccccccccc}
\nu & \cdot & \cdot & -x_1 & -x_1 & x_2 & \cdot & x_3 & \cdot \\
\cdot & \nu & \cdot & x_1 & \cdot & -x_2 & -x_2 & \cdot & x_3 \\
\cdot & \cdot & \nu & \cdot & x_1 & \cdot & x_2 & -x_3 & -x_3 \\
1 & \cdot & \cdot & \cdot & \cdot & \cdot & \cdot & \cdot & \cdot \\
\cdot & 1 & \cdot & \cdot & \cdot & \cdot & \cdot & \cdot & \cdot \\
\cdot & \cdot & 1 & \cdot & \cdot & \cdot & \cdot & \cdot & \cdot \\
\cdot & \cdot & \cdot & 1 & 1 & \cdot & \cdot & \cdot & \cdot \\
\cdot & \cdot & \cdot & \cdot & \cdot & 1 & 1 & \cdot & \cdot \\
\cdot & \cdot & \cdot & \cdot & \cdot & \cdot & \cdot & 1 & 1 \\
\cdot & \cdot & \cdot & x_1 & \cdot & -x_2 & \cdot & \cdot & \cdot \\
\cdot & \cdot & \cdot & \cdot & x_1 & \cdot & \cdot & -x_3 & \cdot \\
\cdot & \cdot & \cdot & \cdot & \cdot & \cdot & x_2 & \cdot & -x_3
\end{array}\right]
\left[\begin{array}{c}
e_1 \\ e_2 \\ e_3 \\ \phi_{12} \\ \phi_{13} \\ \phi_{21} \\ \phi_{23} \\ \phi_{31} \\ \phi_{32}
\end{array}\right]
\tag{B.4}
$$

B.3. Redundancy in specifying all elements of $\hat{e}$

Whenever it is assumed that risk groups do not change size, G rows of the form shown in Eq. (A.11) are added to $\boldsymbol{b}$ and A:

$$
\boldsymbol{b} = \left[\begin{array}{c} \nu x_1 \\ \nu x_2 \\ \nu x_3 \end{array}\right]; \qquad A = \left[\begin{array}{ccccccccc}
\nu & \cdot & \cdot & -x_1 & -x_1 & x_2 & \cdot & x_3 & \cdot \\
\cdot & \nu & \cdot & x_1 & \cdot & -x_2 & -x_2 & \cdot & x_3 \\
\cdot & \cdot & \nu & \cdot & x_1 & \cdot & x_2 & -x_3 & -x_3
\end{array}\right] \tag{A.11}
$$

After multiplying by $\boldsymbol{\theta}$, these G rows can be row-reduced by summing to obtain:

$$
\begin{aligned}
[\nu x_1 + \nu x_2 + \nu x_3] &= [\nu e_1 + \nu e_2 + \nu e_3 + 0\,\phi_{12} + 0\,\phi_{13} + 0\,\phi_{21} + 0\,\phi_{23} + 0\,\phi_{31} + 0\,\phi_{32}] \\
\nu\,[x_1 + x_2 + x_3] &= \nu\,[e_1 + e_2 + e_3]
\end{aligned} \tag{B.5}
$$

which therefore implies that $\sum_i x_i = \sum_i e_i$, or equivalently $\sum_i \hat{x}_i = \sum_i \hat{e}_i = 1$. Thus, it is redundant to specify all G elements of $\hat{e}$, as the final element will be dictated by constant group size constraints.

B.4. Factors of Incidence

Rearranging the force of infection λ_i to isolate the dynamic (not constant) component $(*)$:

$$
\begin{aligned}
\lambda_i &= C_i \sum_k \rho_{ik} \beta \frac{\mathcal{I}_k(t)}{\mathcal{X}_k} \\
&= C_i \beta \sum_k \frac{C_k \mathcal{X}_k}{\sum_{\mathrm{k}} C_{\mathrm{k}} \mathcal{X}_{\mathrm{k}}} \frac{\mathcal{I}_k(t)}{\mathcal{X}_k} \\
&= C_i \beta \underbrace{\frac{\sum_k C_k \mathcal{I}_k(t)}{\sum_{\mathrm{k}} C_{\mathrm{k}} \mathcal{X}_{\mathrm{k}}}}_{*}
\end{aligned} \tag{B.6}
$$

This component $(*)$ is: $\boldsymbol{C}_{\mathcal{I}}$ *the proportion of available partnerships which are offered by infectious individuals.* As the only dynamic component, only this component can be affected by turnover.

Now consider that $\boldsymbol{C}_{\mathcal{I}}$ can be written in terms of the following three factors:

- The average contact rate among infectious individuals $\hat{C}_{\mathcal{I}} = \frac{\sum_k C_k \mathcal{I}_k}{\sum_k \mathcal{I}_k}$
- The proportion of the population who are infectious (prevalence) $\hat{\mathcal{I}} = \frac{\sum_k \mathcal{I}_k}{\sum_k \mathcal{X}_k}$
- The average contact rate among all individuals (constant) $\hat{C} = \frac{\sum_k C_k \mathcal{X}_k}{\sum_k \mathcal{X}_k}$

$$\begin{aligned} \boldsymbol{C}_{\mathcal{I}} &= \hat{C}_{\mathcal{I}} \times \hat{\mathcal{I}} \times \hat{C}^{-1} \\ &= \frac{\sum_k C_k \mathcal{I}_k}{\sum_k \mathcal{I}_k} \times \frac{\sum_k \mathcal{I}_k}{\sum_k \mathcal{X}_k} \times \frac{\sum_k \mathcal{X}_k}{\sum_k C_k \mathcal{X}_k} \\ &= \frac{\sum_k C_k \mathcal{I}_k}{\sum_{\mathrm{k}} C_{\mathrm{k}} \mathcal{X}_{\mathrm{k}}} \end{aligned} \tag{B.7}$$

Therefore, actually only two dynamic factors control the force of infection: 1) the average contact rate among infectious individuals $\hat{C}_{\mathcal{I}}$, and 2) the proportion of the population who are infectious $\hat{\mathcal{I}}$; and the product of these factors (scaled by $\hat{C}^{-1}$) gives $\boldsymbol{C}_{\mathcal{I}}$. Overall incidence is then directly proportional to $\boldsymbol{C}_{\mathcal{I}}$, following Eq. (B.6). In fact, the incidence in each group individually is proportional to $\boldsymbol{C}_{\mathcal{I}}$, as C_i is only factor depending on i.

C. Supplemental Results

C.1. Equilibrium Incidence

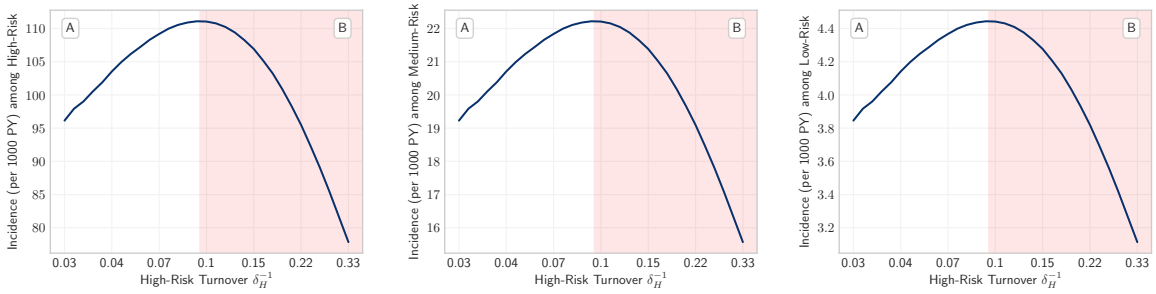

(a) High risk (b) Medium risk (c) Low risk

Figure C.1: Equilibrium incidence among high, medium, and low risk groups versus turnover, as controlled by the duration in the high risk group δ_H. Turnover shown in log scale. incidence in each risk group is proportional to overall incidence with C_i as a scale factor.

C.2. Equilibrium Incidence Ratios

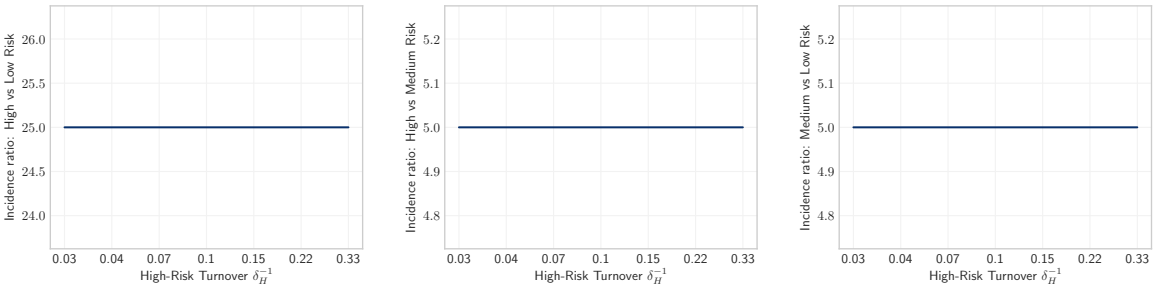

(a) High vs Low risk (b) High vs Medium Risk (c) Medium vs Low Risk

Figure C.2: Equilibrium incidence ratios between risk groups under different rates of turnover ϕ. Incidence ratios do not depend on turnover.

C.3. Equilibrium prevalence before and after model fitting

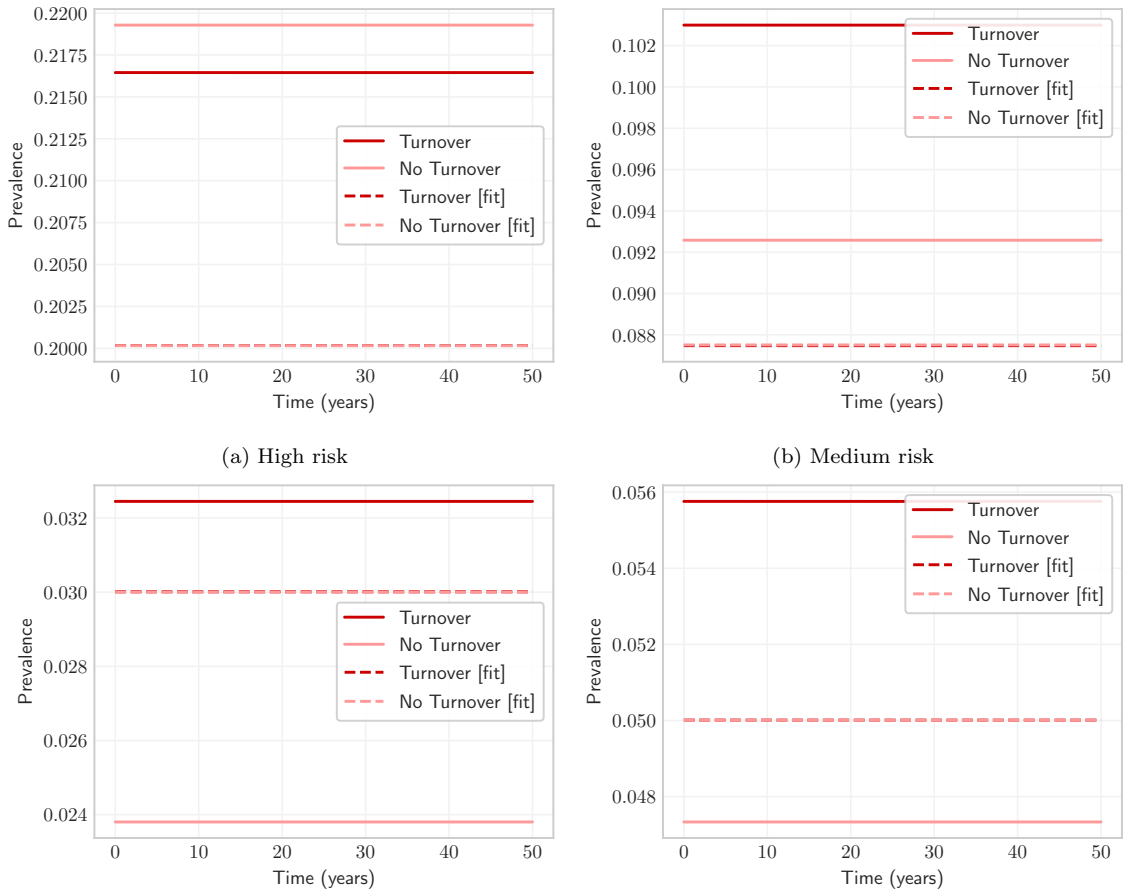

(a) High risk

(b) Medium risk

(c) Low risk

(d) Overall

Figure C.3: Equilibrium STI prevalence among high, medium, and low risk groups as well as overall, with and without turnover, and with and without fitted C_i to group-specific prevalence.

C.4. Contact rate before and after model fitting

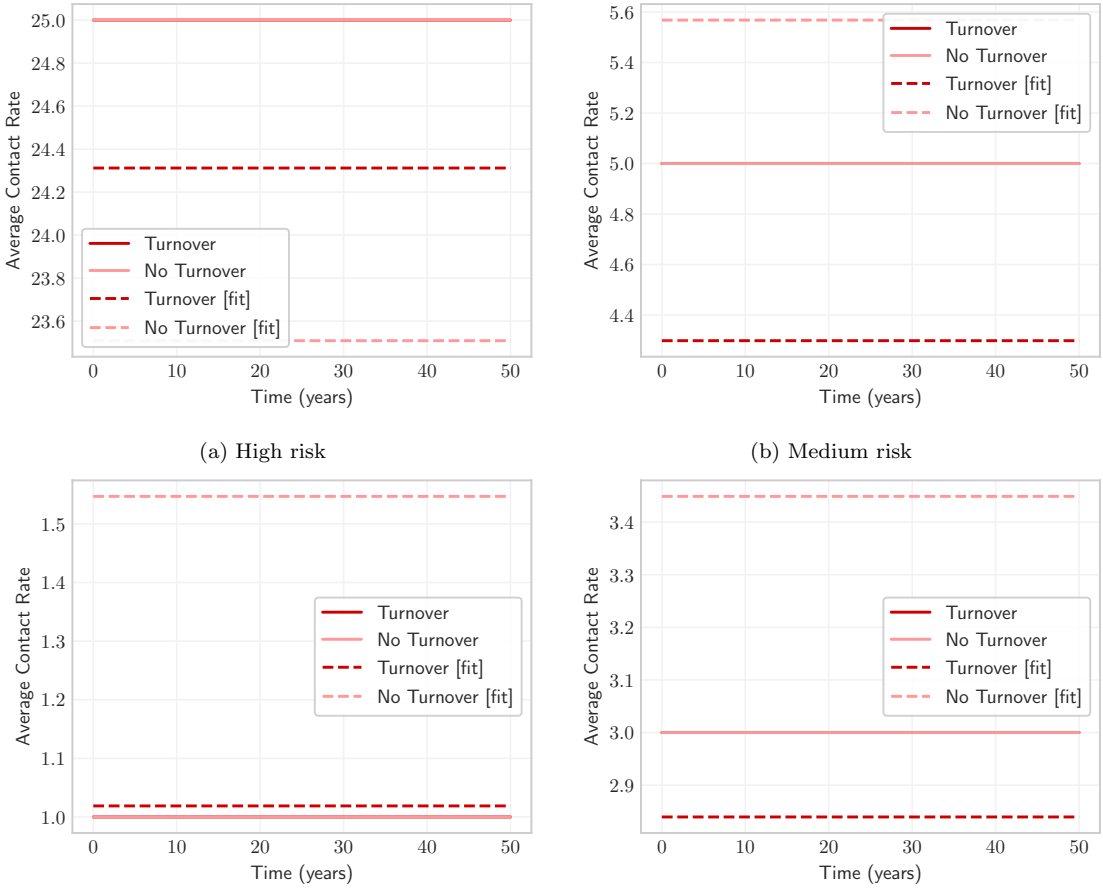

(a) High risk

(b) Medium risk

(c) Low risk

(d) Overall

Figure C.4: Contact rates C_i among high, medium, and low risk groups as well as overall, with and without turnover, and with and without model fitting to group-specific prevalence.

C.5. Influence of turnover on the TPAF of the highest risk group before model fitting

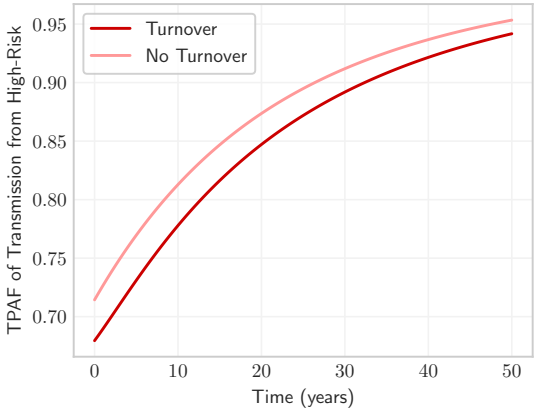

Figure C.5: Transmission population attributable fraction (TPAF-from) of the high risk group in models with and without turnover, before model fitting.

C.6. Distribution of health states at equilibrium

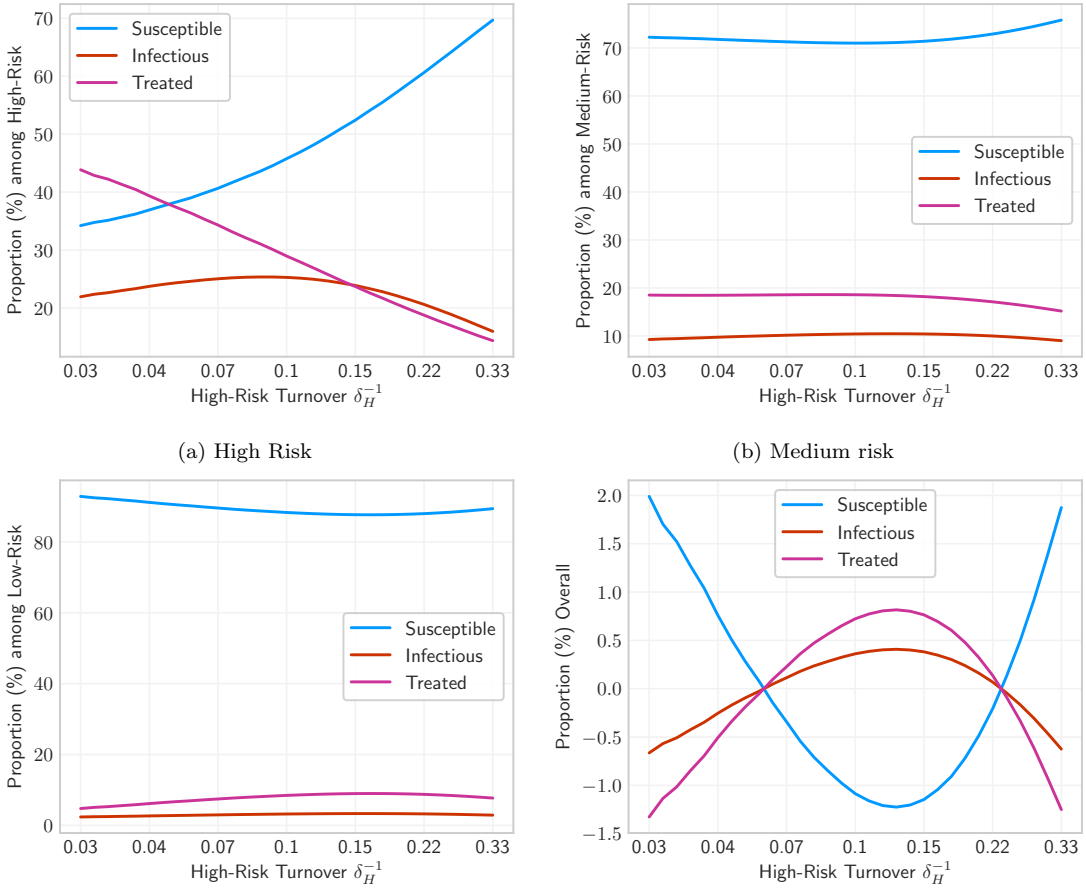

(a) High Risk

(b) Medium risk

(c) Low Risk

(d) Overall

Figure C.6: Equilibrium health state proportions under different rates of turnover.

C.7. Rates of transition at equilibrium

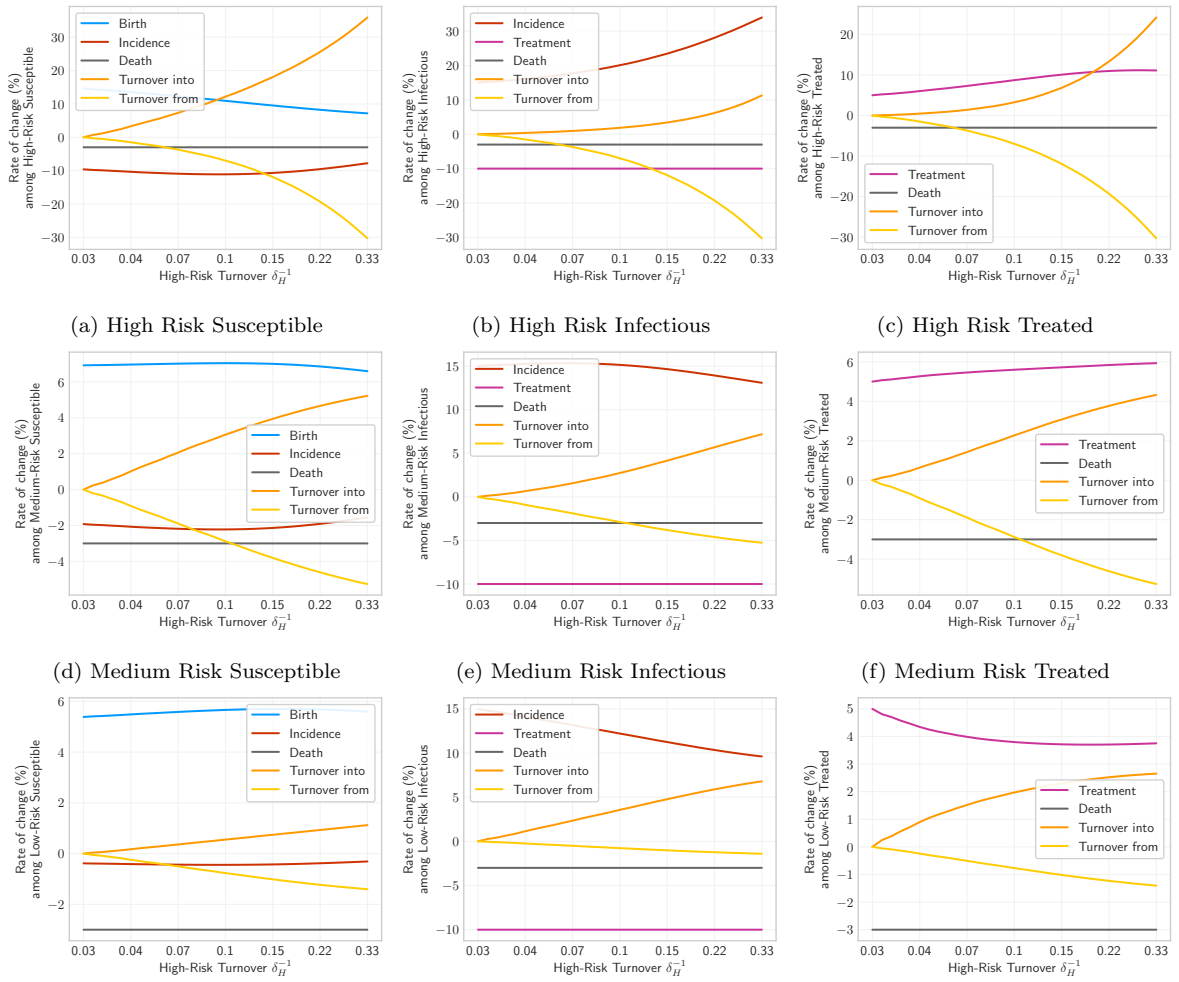

(a) High Risk Susceptible (b) High Risk Infectious (c) High Risk Treated

(d) Medium Risk Susceptible (e) Medium Risk Infectious (f) Medium Risk Treated

(g) Low Risk Susceptible (h) Low Risk Infectious (i) Low Risk Treated

Figure C.7: Rates of transition among risk groups and health states at equilibrium. All transition rates are shown relative to the named group, for both afferent and efferent transitions. Although each system is at equilibrium, profiles should not sum to zero due population growth.

C.8. New infections from turnover vs incidence

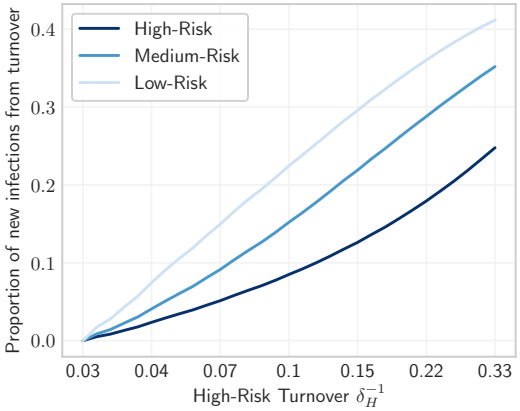

Figure C.8: Proportion of new infectious individuals in each risk group which are from turnover of infectious individuals, as opposed to infection of susceptible individuals in the risk group ($\tau = 0.1$).